ICE: A Low-Cost IoT Platform Targeting Real-Time Anonymous Visitors Flow Tracking at Museums

Vasileios Serasidis
Dept. of Physics
Aristotle University of Thessaloniki
Thessaloniki, Greece

Ioannis Sofianidis
Dept. of Physics
Aristotle University of Thessaloniki
Thessaloniki, Greece

Giorgos Margaritis
Dept. of Physics
Aristotle University of Thessaloniki
Thessaloniki, Greece

Christos Sad
Dept. of Physics
Aristotle University of Thessaloniki
Thessaloniki, Greece

Vasileios Konstantakos
Dept. of Physics
Aristotle University of Thessaloniki
Thessaloniki, Greece

Kostas Siozios
Dept. of Physics
Aristotle University of Thessaloniki
Thessaloniki, Greece

2023 IEEE 32nd International Symposium on Industrial Electronics (ISIE) | 979-8-3503-9971-4/23/$31.00 ©2023 IEEE | DOI: 10.1109/ISIE51358.2023.10228181

***Abstract*—Museums are uniquely positioned to blend education and recreation in ways that can both challenge and catalyze communities. During the last years, IoT technology has revolute the way that museums enable visitors to engage with cultural institutions. Among others, sensor-based technology enables museums to provide visitor flow solutions that provide smart people tracking. Typically these systems rely to Bluetooth and WiFi beacons with accuracy around 1 meter. Throughout this paper, we introduce a low-cost IoT platform that relies on Ultra-WideBand technology to enable real-time accurate indoor positioning and navigation. Experimental results with different scenarios highlight the superiority of proposed platform, since the mean error between estimated and actual path can be up to 15cm, which in turn is sufficient to enable new services to museums of the future.**

***Index Terms*—Low-cost, IoT, Indoor positioning.**

I. Introduction

Museums today face both overt and subtle challenges. The traditional model of the museum experience as passive observation is decisively shifting to active, interpretive engagement. Exhibits are no longer framed by expert appreciation; instead, they acknowledge the subjectivity of multiple perspectives. This emerging mode is particularly evident in the popularity of interdisciplinary and inter-institutional collaborations. Museums are rethinking and reworking their spaces to promote deeper understanding of their collections and missions, greater interactivity, a fuller range of activities, and increased revenue stability. During the last years, there were varied ideas about how audiences expect to engage with cultural institutions. Among others, technology solutions that enable visitor flow tracking is of upmost importance, as this new feature enables numerous services. In detail, museums are using visitor flow technology to understand how people experience their exhibits. The data is used to improve the visitor experience by providing content that aligns with visitors' interests and helping museums organize their collections in a way that better connects with visitors' needs [7]. This new approach has changed the museum landscape forever.

In more detail, visitors' flow tracking technologies enable more advanced, or even fully customised, tour scenarios. By the term scenario we mean a sequence of proposed tour steps. Each step of the tour may be either a transition to an exhibit or more generally to an information point. Hence, it is feasible to enable an organization to design various dynamic tour scenarios (that might vary, and they can be changed, modified or increased by the administrator) based on the available time, the themes and the preferences of the visitors. Also, the map application is one of the most important characteristics of a multimedia tour system, providing crucial guidance and information about the surrounding exhibits and points of interest. This information can be combined to a graphic floor plan helps visitors understand their position in the building and its areas. The map feature can also be used as the basis for tour scenarios with criteria such as available time and preferred thematic content. Last but not least, by combining such systems with audio devices it is possible to enable addition of specialized applications for people with disabilities (e.g. vision problems).

The data of such a system is crucial also for the organization to generate statistical data and reports for analysis, which in turn provides valuable information regarding site operations and visitor preferences on the following: (i) *traffic*: records information about the number of visitors, their chronological distribution, and other characteristics of the system, and (ii) *exhibit viewing* that tracks viewing choices and time spent in different exhibits or areas.

During the last decade various indoor positioning systems that rely on WiFi [1] and Bluetooth [2] beacons, have been presented. The operation of these systems is based on RSSI (Received Signal Strength Indicator) feature vector [8] composed of received signal values from different emitting devices, or beacons. In case we also consider the position of beacon deployment, the previously mentioned technologies enable also proximity functionality. Apart from these technologies,

This research has been co-financed by the European Regional Development Fund of the European Union and Greek national funds through the Operational Program Competitiveness, Entrepreneurship and Innovation, under the call RESEARCH – CREATE – INNOVATE (project code: T2EDK-02564).

GPS-based solutions [3] are also used for this purpose, but with limited efficiency due to attenuation of the satellite signal to indoor environments.

Although the previous mentioned systems support indoor positioning in room-scale, however their main drawback affects their limited accuracy, which ranges between 1-4 meters depending on the implementation's complexity. To overcome this drawback, algorithms that improve accuracy were also explored [2] [1]. However, these algorithms have increased computational complexity; thus, their execution cannot be performed onto low-cost embedded devices. Apart from them, solutions that rely on Ultra-WideBand (UWB) technology, have also been proposed [8] [10].

Throughout this paper, we introduce an indoor positioning system to enable real-time anonymizes visitors flow tracking at museums. The proposed solution relies on a UWB technology that enables higher precision positioning as compared to existing solutions. Experimental results with different operating configuration scenarios and indoor trajectories highlight the superiority of introduced solution, as we achieve on average accuracy ranging between 5–7cm. Additionally, the proposed IoT platform exhibits limited computational and storage complexities; thus, its functionality is demonstrated as part of a low-cost embedded device with limited maintenance cost (e.g. power charges).

The rest of the paper is organized, as follows: Section II describes the proposed architecture for the indoor positioning solution. The algorithmic approach for this system is discussed in Section III. Experimental results that highlight the efficiency of the proposed solution as compared to state-of-the-art relevant products are provided at Section IV. Finally, Section V concludes the paper.

II. Architecture of Proposed IoT System

This section describes the architecture of the proposed low-cost IoT system for indoor positioning and navigation. Three types of nodes are used for this purpose, namely (i) the `anchors`, (ii) the `tags` and (iii) the `local hub`.

In detail, anchors are electronic devices that send out Ultra-WideBand (UWB) blinks that are received by UWB tags. To cover the area with an indoor tracking system, a set of anchors needs to be installed above the area to create the location infrastructure. Regarding the tags, they are small electronic devices that are curried by museum's visitors. Each tag detect UWB pulses emitted by UWB anchors and performs trilateration to perform positioning service. Then, the results are forwarded to the local hub to enable further processing. For this purpose, IEEE 802.15.1 protocol is employed. Each anchor and tag is equipped with a high-performance omnidirectional UWB antenna provides a uniform omnidirectional pattern resulting in an equal true 360° range. Consequently, there is no need for device orientation adjustments, which is crucial, especially once the anchor is deployed and becomes physically unreachable. Finally, the system is fully scalable, allowing unlimited expansion of the tracking area just by adding extra anchors to the network. Also, the employed algorithm for distance calculation (that will be discussed in upcoming section) can track an unlimited number of tags within the system and thousands of them within a single area for tracking visitors at museums.

The system's installation phase impose to assign anchors to predefined locations (x and y coordinates in room scale), while tag(s) can be randomly moved within this area. In order to maximize the accuracy, anchors location should be carefully selected to support sufficient area coverage. Based on our exploration, we conclude that 4 – 6 anchors should be placed per room. These anchors should be uniformly distributed over the room's area by taking into consideration the phenomena of reflection, refraction, diffraction, absorption, and scattering (e.g. from dark points) [5].

A. Calculate Time-of-Flight

Positioning systems that rely on beacon technology perform distance calculation between anchors and tag based on time-of-flight (ToF) metric, which is proportional to the distance (in meters) between tag and anchor. Widely adopted solutions for this purpose include among others *time-of-arrival* (ToA) and *time-difference of arrival* (TDoA) techniques. More precisely, the ToA technique measures the time elapsed from message transmission (source node) until it is received (target node). Similarly, at the TDoA approach anchors transit periodically messages and the tag calculate the time difference between consecutive received messages. Both techniques exhibit increased design complexity, since they assume clocks synchronization among devices (even a negligible offset in clocks might result to hundreds of meters accuracy loss), which is not trivial for low-cost solutions.

On the other hand, the proposed localization service relies on Two-Way-Ranging (TWR) technique, depicted schematically at Figure 1. Since this approach does not distinguish between transmitter and receiver node, both tag and anchors transmit and receive messages. Without affecting the general applicability of this approach, we will assume that the tag (visitor) initiates periodically a task for positioning estimation. For this purpose, it broadcasts a packet that contains tag's unique ID (*tag_id*) and timestamp t_1 (refers to the time of transmission). In case an anchor receives such a packet, it replies by attaching its own unique ID (*anchor_id*), the time of packet's receipt (timestamp t_2), as well as the time of new transmission (timestamp t_3). Finally, in case a tag receives anchor's transmission, it checks whether its own id (*tag_id*) can be found inside the packet. If yes, it attaches the current timestamp (t_4) and the packet is further processed in order to calculate the time-of-flight (ToF) based on Equation 1.

$$ToF = \frac{(t_4 - t_1) - (t_3 - t_2)}{2} \tag{1}$$

B. Data transfer mechanism

This subsection describes the proposed protocol, depicted at diagram level at Figure 2, that performs data exchange from tags to local hub. The functionality of this protocol is

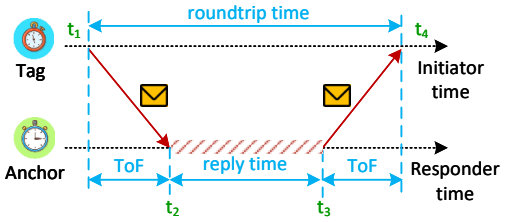

Fig. 1: Overview of the employed technique for calculating distance between tag and anchor.

completely reactive, as it waits for the arrival of any packet to be processed. Our approach supports five packet types, as they are summarized at Table I. Specifically, in case the packet type is *HELLO*, then the corresponding acknowledge (*ACK*) packet is created that contains information about the employed DATA packet size (depending on the link's implementation), as well as its origin and destination nodes. The *START* and *STOP* packets denote the starting and stop of data transfer procedure between source and destination nodes. The localization information is transmitted with *DATA* packets, while control messages (e.g. link configuration, desired link speed, selected encryption scheme, etc) are sent in *CONTROL* packets. As a response to these packets, the node confirms their proper receive with an *ACK* packet.

TABLE I: Packets of the proposed communication protocol.

Type of packet	Description
P_HELLO	This packet discovers the network.
P_START	The P_START packet is used for establishing the connection.
P_STOP	It is used for terminating the connection.
P_CONTROL	Includes control messages for operating device and link.
P_DATA	It contains data about the current position, as well as all the necessary redundant data for error correction. Note that P_DATA packets can be adapted to carry even more information.
P_ACK	This packet acknowledges the successful receipt of packet.

Throughout this paper, we applied the previously mentioned communication scheme as part of the underline IEEE 802.15.1 protocol in order to support the data transfers between tags and local hubs. The selection of this protocol is based on its widely acceptance for short and medium range connectivity among nodes with energy efficiency and limited demand for throughput. In order to highlight and quantify the flexibility of the employed interconnection scheme, Figures 3(a) and 3(b) plot the variation of transmission time for different configurations of IEEE 802.15.1 protocol. Specifically, Figure 3(a) refers to a case that only one tag transmits data, while at the latter approach considers multiple tags (ranging between 2 and 6) that are transmitting simultaneously.

Based on this analysis, we conclude that the increase of packet size results to a significant reduction at transmission time. Moreover, Figure 3(a) indicates that the increase of time internal (i.e. the time between two consecutive packet transmissions) has almost negligible impact at the overall transmission time. Thus, depending on the constraints posed by the target usecase, the designer is able to select the proper configuration of communication links. It is well-worth to mention also that as we increase the number of tags that send simultaneously data, there is almost no penalty at total transmission time. This occurs mainly due to the incorporated conflict alleviation mechanisms found in IEEE 802.15.1 protocol. Regarding the scopes of our implementation, we enable the dynamic modification of packet size depending on the number of nodes per link and the amount of data to be transmited. This task is realized with *CONTROL* packets.

III. Indoor Positioning

Having as input the distances from tag to room's tags (as they are were computed based on ToF metric with Equation 1), this section describes the calculation of tag's (x, y) location within a room. Our system applies the trilateration method, which calculates the Cartesian coordinates of tag based at least on 3 reference points (anchors). For demonstration purposes, lets assume that our architecture consists of 1 tag and 3 anchors (marked with A, B and C), as it is depicted at Figure 4. In such a case, the radius of each circle (Euclidean distance) is computed according to Equations 2–4.

$$r1 = \sqrt{(x - x_1)^2 + (y - y_1)^2} \tag{2}$$

$$r2 = \sqrt{(x - x_2)^2 + (y - y_2)^2} \tag{3}$$

$$r3 = \sqrt{(x - x_3)^2 + (y - y_3)^2} \tag{4}$$

In order to solve these equations, we apply the least squares error method, which exhibits limited computational complexity and can be deployed in low-performance embedded devices. More specifically, the previously mentioned equations can be represented in the following form:

$$(x-x_1)^2+(y-y_1)^2-[(x-x_2)^2+(y-y_2)^2] = r_1^2-r_2^2 \tag{5}$$

$$(x-x_1)^2+(y-y_1)^2-[(x-x_3)^2+(y-y_3)^2] = r_1^2-r_3^2 \tag{6}$$

Hence, the Equations 5 and 6 cane be represented in the form of tables $Ax = b$, as it is depicted at Equation 7. The solution of this equation is retrieved according to $X = A^{-1}b$. In case, the system has more anchors ($A1$, $A2$, ..., Ax) than tags, the tag's position is calculated based on $X = (A^T A)^{-1} A^T b$.

$$\underbrace{2\begin{pmatrix} x_2 - x_1 & y_2 - y_1 \\ x_3 - x_1 & y_3 - y_1 \end{pmatrix}}_{A} \times \underbrace{\begin{pmatrix} x \\ y \end{pmatrix}}_{X} = \underbrace{\begin{pmatrix} r_1^2 - r_2^2 - x_1^2 - y_1^2 + x_2^2 + y_2^2 \\ r_1^2 - r_3^2 - x_1^2 - y_1^2 + x_3^2 + y_3^2 \end{pmatrix}}_{b} \tag{7}$$

The accuracy of tag's positioning can be further improved with the iterative least squares (RLS) method. In detail, RLS is an adaptive filter algorithm that iteratively finds the coefficients that minimize a weighted linear least squares cost function relating to the input signals. In order to implement this method, initially we assume that tag's location is (X_p, Y_p), where the distance from all the anchors is the same (as it is

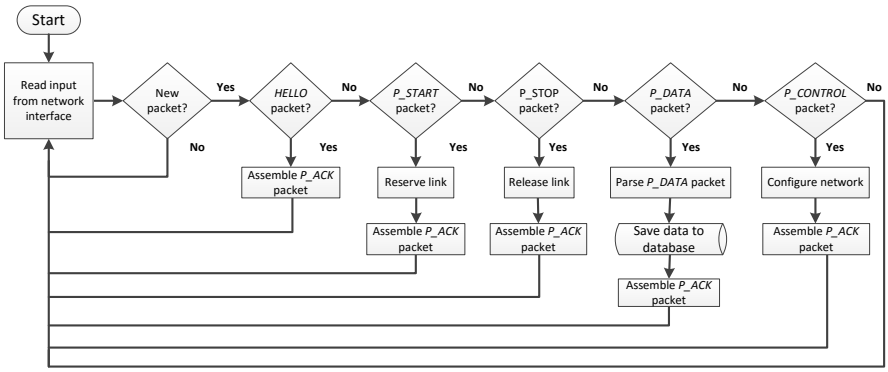

Fig. 2: Dataflow for the employed communication protocol.

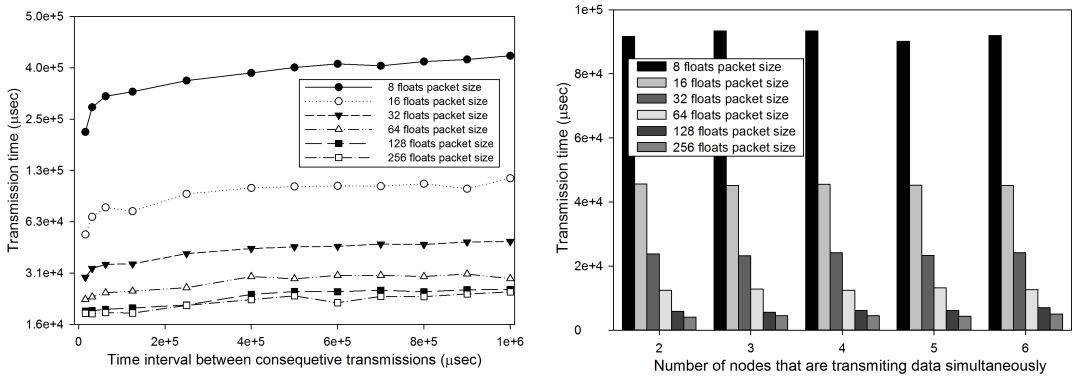

Fig. 3: Transmission time for (a) a single tag that sends packets with different sizes and (b) multiple tags.

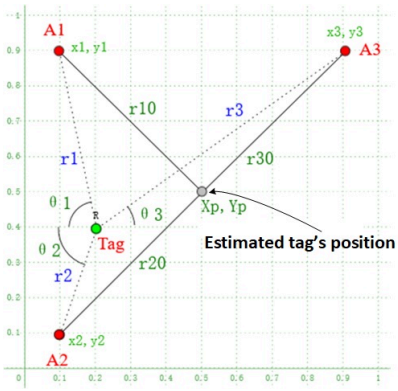

Fig. 4: Positioning estimation based on trilateration method.

depicted at Figure 4. Next, we summarize the sine and cosine for angles θ_1, θ_2, and θ_3. Also, we calculate the difference between radius $r1 - r10$, $r2 - r20$, and $r3 - r30$ found in table b. These data are fed to the least square algorithm in order to calculate the anchor's deviation versus its previous positioning (X_p, Y_p). Finally, we refine tag's position and repeat iteratively algorithm until the error to be minimized (the values of array b to be minimized). For demonstration purposes, the previously mentioned analysis refers to a case with 3 anchors and 1 tag; however, it is also applicable to any other system configuration. The pseudocode depicted at Algorithm 1 implements the functionality of calculating tag's position with the proposed framework.

To further improve the accuracy of our system, we apply a complementary filter, which consists of a combination of

Algorithm 1 Proposed algorithm for indoor positioning.

Require: $max\_iterations \geq 0$
  while ($i \neq max\_iterations$) **do**
    $r10 \leftarrow \sqrt{(Xp - X1)^2 + (Yp - Y1)^2}$
    $r20 \leftarrow \sqrt{(Xp - X2)^2 + (Yp - Y2)^2}$
    $r30 \leftarrow \sqrt{(Xp - X3)^2 + (Yp - Y3)^2}$
    $A \leftarrow [\frac{Xp-X1}{r1} * \frac{Yp-Y1}{r1}; \frac{Xp-X2}{r2} * \frac{Yp-Y2}{r2}; \frac{Xp-X3}{r3} * \frac{Yp-Y3}{r3}]$
    $b \leftarrow [r1 - r10; r2 - r20; r3 - r30]$
    $X \leftarrow \frac{1}{(A' * A)} * (A' * b)$
    $Xp \leftarrow Xp + X(1)$
    $Xp \leftarrow Xp + X(2)$
    if (b improvement is negligible) **then**
      stop iterations
    end if
  end while

a Low-Pass Filter (LPF) and a High-Pass Filter (HPF). Such a min-max approach reduces signal noise towards improving the accuracy of localization estimations. The efficiency of this filter depends on the a parameter (in the range of [0, 1]), which defines that the algorithm will compute current output based on $(1 - a)\%$ of the previous value increased by $a\%$ of the current value. Previous studies indicate that complementary filter outperforms the corresponding accuracy from Kalman filter, while it also exhibit less computational complexity [4].

IV. Experimental results

The proposed indoor positioning system was implemented based on DWM1001-DEV development board that rely on UWB technology [6], while the data processing is performed within tag (at a Raspberry Pico processing node). For evaluation purposes, the system consisted of up to 6 anchors and 1 tag that were installed to a large-scale. The efficiency of the proposed solution was evaluated with three representative scenarios (i.e. movements) within a room, namely a *diagonal*, a *zig-zag*, and a *random* path.

A. Diagonal Path

The efficiency of the proposed indoor positioning system was initially evaluated based on a diagonal path. The results to this analysis (output of trilateration method) regarding both the raw data and the proposed positioning framework (based on iterative mean square error and complementary filter) are depicted at Figure 5 with red- and purple-colored lines, respectively. At this figure we depict also with green color line the reference solution (ground-truth path).

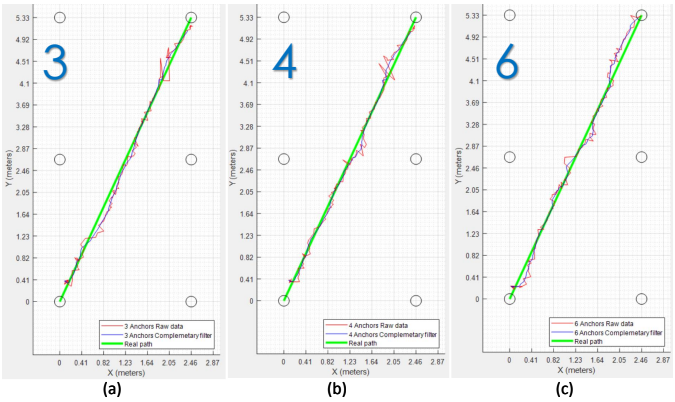

Fig. 5: Accuracy of proposed positioning system with 3, 4, and 6 anchors vs. ground-truth regarding the diagonal path.

Although the diagonal path is the simplest one among the studied flow tracking scenarios, it is used in order to quantify the efficiency of our platform to perform indoor localization based on different number of available anchors. For this purpose, we explore the accuracy of positions when the localization algorithm considers only the 3 and 4 closest anchors (based on the time-of-flight metric), as well as in case it received UWB blinks for all the available anchors. Based on this analysis, as it is summarized at Table III, the proposed solution results to an accuracy displacement ranging from 3–4.8cm, on average.

B. Zig-Zag Path

Next, we consider a zig-zag pattern to evaluate system's response at frequent changes to the tag's direction. The results to this analysis regarding both the raw data, as well as the proposed positioning framework are depicted at Figure 6. In detail, this analysis highlight results both for the iterative mean square error (red color) and the complementary filter (purple color). The reference to this analysis is the ground-truth path depicted with green color line.

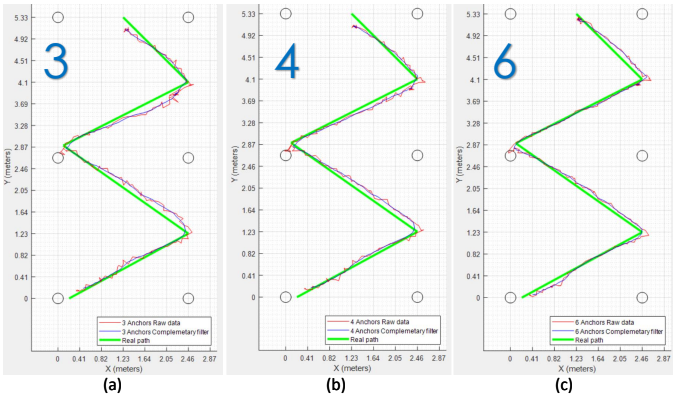

Fig. 6: Accuracy of proposed positioning system with 3, 4, and 6 anchors vs. ground-truth regarding the zig-zag path.

For sake of completeness we also explore the same scenario when the positioning algorithm considers fewer anchors. For this purpose, visitors flow is conducted when we consider data from the 3 and 4 closest anchors to the tag (based on the time-of-flight metric). The results from this analysis are summarized at Table III. Based on this analysis, we conclude that the proposed system achieves superior performance for all the studied configuration setups. Specifically, we improve both minimum and maximum error for the whole path, which range from 0.013cm up to 15cm. Also, standard deviation metric also confirms this superiority, as the values range from 4.3cm (regarding 3 anchors) up to 3.39cm (for 6 anchors).

C. Random Path

Finally, we evaluate also the efficiency of the proposed system with a more complex path, where tag is moved across the whole room. This scenario aims to stress the indoor positioning algorithm with additional turns, as well as movements across different directions. The results of this analysis are visualized at Figure 7. Similar to previous cases, both raw data and data from complementary filter are compared versus the ground-truth path. Additionally, in order to further quantify the efficiency of this case study, Table IV provides the statistical analysis of algorithm's accuracy regarding system configurations where tag considers only 3, 4 and 6 anchors. Similar to previous conclusions, the minimum and maximum error for the proposed indoor positioning system range between 0.015cm and 26cm, respectively. Regarding the mean error, it ranges from 5cm (when only the 3 closest anchors are considered) up to 15cm (for the scenario with 6 anchors).

The previously mentioned analysis indicates that the ICE IoT platform enables accurate visitors flow tracking at indoor environment. In detail, instead of similar existing solutions, that rely either on Bluetooth [1], WiFi [2], or UWB beacons [7] [8] [9], the proposed IoT achieves significant higher precision, as it improves on average the mean error compared to ground-truth trajectory from 30–90cm (as it is reported in

TABLE II: Statistical analysis regarding the diagonal path (error based on ground-truth) in cm.

	Raw	Proposed	Raw	Proposed	Raw	Proposed
Num. Anchors	3	3	4	4	6	6
Min	0.119	0.051	0.038	0.026	0.014	0.013
Max	20.34	11.23	26.36	11.06	19.75	13.16
Mean	5.563	4.224	4.775	3.084	5.661	4.843
Median	5.052	4.261	3.839	2.222	4.106	4.579
Standard deviation	4.128	2.954	4.442	2.767	4.863	3.529

TABLE III: Statistical analysis regarding the zig-zag path (error based on ground-truth) in cm.

	Raw	Proposed	Raw	Proposed	Raw	Proposed
Num. Anchors	3	3	4	4	6	6
Min	0.019	0.013	0.084	0.083	0.035	0.024
Max	26.66	16.89	22.10	14.31	22.06	15.21
Mean	7.746	7.371	7.315	6.848	4.678	3.965
Median	7.608	7.381	7.170	7.484	3.407	3.230
Standard deviation	5.081	4.353	4.171	3.760	4.200	3.390

TABLE IV: Statistical analysis regarding the random path (error based on ground-truth) in cm.

	Raw	Proposed	Raw	Proposed	Raw	Proposed
Num. Anchors	3	3	4	4	6	6
Min	7.381	0.555	0.0161	0.059	0.023	0.015
Max	35.42	26.80	34.50	25.04	85.17	44.61
Mean	5.832	5.640	7.268	7.072	14.48	13.80
Median	4.367	4.601	5.333	5.350	13.01	13.24
Standard deviation	5.310	4.763	6.448	5.422	11.13	9.547

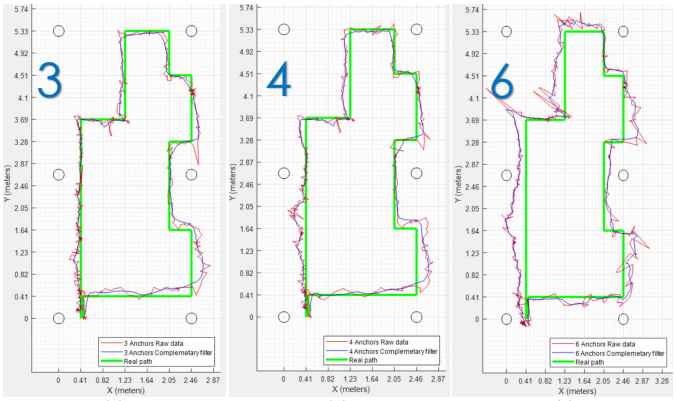

Fig. 7: Accuracy of proposed positioning system with 3, 4, and 6 anchors vs. ground-truth regarding the random path.

state-of-the-art solutions) up to 13 cm regarding the random path. Another competitive advantage of the proposed solution affects the reduced computational and storage complexities; thus, it is possible to be provide real-time services with a low-cost embedded device (the ICE platform relies on a raspberry pico processing node).

V. Conclusions

A novel IoT system that provides indoor positioning, was introduced. The localization feature is supported based on UWB beacon technology to achieve high precision measurements. Apart from hardware aspects, the proposed IoT platform outperforms relevant approaches, as the employed algorithms exhibit significant lower computational complexity, enabling among others real-time execution onto low-cost embedded devices. Experimental results highlighted the superiority of introduced solution, as the mean error between estimated and actual path can be up to 13cm for the representative paths studied throughout this paper.

References

[1] X. Du, K. Yang and D. Zhou, "MapSense: Mitigating Inconsistent WiFi Signals Using Signal Patterns and Pathway Map for Indoor Positioning," in IEEE Internet of Things Journal, vol. 5, no. 6, pp. 4652-4662, Dec. 2018.

[2] L. Bai, F. Ciravegna, R. Bond and M. Mulvenna, "A Low Cost Indoor Positioning System Using Bluetooth Low Energy," in IEEE Access, vol. 8, pp. 136858-136871, 2020.

[3] X. Li, "A GPS-Based Indoor Positioning System With Delayed Repeaters," in IEEE Transactions on Vehicular Technology, vol. 68, no. 2, pp. 1688-1701, Feb. 2019.

[4] Xiaolin Liang, Hao Zhang, Shengbo Ye, Guangyou Fang, T. Aaron Gulliver, "Improved denoising method for through-wall vital sign detection using UWB impulse radar", Digital Signal Processing, Vol. 74, pp 72-93, 2018.

[5] Zou Y, Liu H. TDOA localization with unknown signal propagation speed and sensor position errors. IEEE Communications Letters. 2020 Jan 21;24(5):1024-7.

[6] Qorvo DWM1001-DEV Module Development Board, available online https://www.decawave.com/product/dwm1001-development-board/

[7] Ferrato, Alessio and Limongelli, Carla and Mezzini, Mauro and Sansonetti, Giuseppe, "Using deep learning for collecting data about museum visitor behavior", Applied Sciences, Vol. 12, No. 2, pp. 533, 2022.

[8] A. R. Jiménez and F. Seco, "Finding objects using UWB or BLE localization technology: A museum-like use case," 2017 International Conference on Indoor Positioning and Indoor Navigation (IPIN), Sapporo, Japan, 2017, pp. 1-8.

[9] F. Hachem, D. Vecchia, M. L. Damiani and G. P. Picco, "Fine-grained Stop-Move Detection in UWB-based Trajectories," 2022 IEEE International Conference on Pervasive Computing and Communications (PerCom), Pisa, Italy, 2022, pp. 111-118.

[10] A. Courtay, M. L. Gentil, O. Berder, P. Scalart, S. Fontaine and A. Carer, "Anchor Selection Algorithm for Mobile Indoor Positioning using WSN with UWB Radio," 2019 IEEE Sensors Applications Symposium (SAS), Sophia Antipolis, France, 2019, pp. 1-5.